

W boson mass measurement

N. ANDARI *On behalf of the ATLAS and CMS Collaborations*

Department of Physics and Astronomy, University of Birmingham, B15 2TT, England

I describe the first measurement of the W boson mass at the LHC performed using 4.6 fb^{-1} of proton–proton collision data recorded in 2011 at a centre-of-mass energy of 7 TeV with the ATLAS detector, as well as the W-like Z boson mass measurement performed by the CMS collaboration. The measured W boson mass in ATLAS is $80370 \pm 19 \text{ MeV}$, consistent with the Standard Model prediction and with the world average obtained from the combination of the LEP and Tevatron measurements. The ATLAS result is currently the most precise individual measurement of the W boson mass. The overview of the analyses is given with an emphasis on the ATLAS result.

1 Introduction

The loop-induced radiative corrections to the W boson mass in the electroweak (EW) sector of the Standard Model (SM) ^{1,2,3} are dominated by the running of the electromagnetic coupling due to light-quark loops, and the contribution from top (and bottom) quarks and Higgs bosons loops in the W boson propagator. Therefore, probing the relation between the W boson, top and Higgs boson masses provides a stringent test of the consistency of the SM. The global EW fit predicts $m_W = 80358 \pm 8 \text{ MeV}$ ⁴ setting a natural goal of 8 MeV for the precision of the W boson mass measurement. Currently, the world average value of the W boson mass is $m_W = 80385 \pm 15 \text{ MeV}$ ⁵ obtained from the combination of the LEP and Tevatron results, with the most precise single measurement provided by the CDF collaboration with an uncertainty of 19 MeV ⁶.

The measurement of the W boson mass is particularly challenging at the LHC as compared to the LEP and Tevatron experiments, due to the large number of interactions per beam crossing and to the significant contributions of second-generation quarks to W boson production, where 25% of the inclusive W boson production rate is induced by at least one *s* or *c* quark. Recently, the first measurement of m_W at the LHC collider was performed by the ATLAS collaboration ^{7,8}, using data recorded in 2011 at a centre-of-mass energy of 7 TeV. The W boson decays into an electron or muon and a neutrino are considered. The mass is obtained by reconstructing the Jacobian edges of the final-state kinematic distributions, the transverse momentum of the charged lepton and the W boson transverse mass. The measurement requires an accurate calibration of the detector response and a well defined physics modelling. A W-like measurement of the Z boson mass using dimuon events collected in proton–proton collisions at a centre-of-mass energy of 7 TeV was performed by the CMS collaboration ^{9,10} as a first step towards a W boson mass measurement.

An overview of the W boson mass measurement in ATLAS is given, the strategy is described in section 2, the experimental aspects of the measurement are discussed in section 3, the theoretical ones are discussed in section 4. Section 5 summarises the results of the Z boson mass measure-

ments in ATLAS and CMS, the W boson mass measurement in ATLAS and the corresponding uncertainties.

2 Strategy of the measurement

Since it is not possible to fully reconstruct the W boson mass, the measurement relies on mass-sensitive final state variables, the transverse momentum of the charged lepton p_{T}^{ℓ} and the W boson transverse mass m_{T} . m_{T} is commonly defined as $m_{\text{T}} = \sqrt{2p_{\text{T}}^{\ell}p_{\text{T}}^{\text{miss}}(1 - \cos\phi)}$ where $p_{\text{T}}^{\text{miss}}$ is the neutrino missing transverse momentum and ϕ is the opening azimuthal angle between the charged lepton and missing transverse momenta. The neutrino missing transverse momentum is defined as $\vec{p}_{\text{T}}^{\text{miss}} = -(\vec{u}_{\text{T}} + \vec{p}_{\text{T}}^{\ell})$, the hadronic recoil, \vec{u}_{T} , being the vector sum of the transverse energy of all clusters reconstructed in the calorimeters excluding the lepton deposits. Predictions of these final-state distributions for different values of m_{W} are obtained by reweighting the W boson invariant mass distribution in the simulated reference sample according to a Breit-Wigner distribution. These distributions, referred to as templates, are compared to the observed distributions and a χ^2 minimisation is performed to extract the best fit template and the corresponding measured W boson mass.

The event selection requires exactly one reconstructed lepton (electron or muon) in the detector acceptance with $p_{\text{T}}^{\ell} > 30$ GeV, passing identification and isolation criteria. The leptons are required to match the corresponding trigger selection. In addition, the following cuts are applied: $u_{\text{T}} < 30$ GeV, $p_{\text{T}}^{\text{miss}} > 30$ GeV and $m_{\text{T}} > 60$ GeV. With these selections, a total of 5.89×10^6 of W boson candidates are selected in the electron decay channel and 7.84×10^6 in the muon decay channel.

The final W boson mass is obtained from the combination of the electron and muon decay channels and of the charges and lepton pseudorapidity (η) categories. Fitting ranges of $32 < p_{\text{T}}^{\ell} < 45$ GeV and $66 < m_{\text{T}} < 99$ GeV, optimised to minimise the total expected measurement uncertainty, are used to derive the W boson mass. The Z boson sample is used to validate the analysis and to provide significant experimental (lepton and recoil calibration) and theoretical constraints (using ancillary measurements).

3 Experimental precision

3.1 Lepton calibration

The procedures used in the W mass analysis for lepton calibration rely mainly on the published results by ATLAS^{11,12}, based on W and Z samples at centre-of-mass energies of 7 and 8 TeV. Lepton momentum and energy corrections are derived exploiting the precisely measured value of the Z boson mass at LEP¹³. Identification and reconstruction efficiency corrections are derived from W and Z boson events using the tag-and-probe method.

Muon momentum scale and resolution corrections are derived using $Z \rightarrow \mu\mu$ decays. The linearity of the scales is checked by probing the muon momentum scale corrections as a function of $1/p_{\text{T}}$ of the muons in various η ranges. The remaining non-linearity is considered as a systematic uncertainty and dominates the systematic uncertainty in the muon momentum scale. The systematic uncertainty in the resolution corrections is dominated by the statistical uncertainty of the Z boson sample.

Sagitta bias corrections are derived from the combination of two methods using the peak of the invariant mass distribution in $Z \rightarrow \mu\mu$ events and the ratio of the measured energy in the calorimeter to the electron momentum measured in the inner detector in $W \rightarrow e\nu$ events. The combined uncertainty is dominated by the finite size of the Z boson sample. The muon efficiency

corrections are derived as a function of p_T^ℓ and η separately for positive and negative charges. The dominant uncertainty is the statistical uncertainty of the Z boson sample.

Combining the different η categories, the total muon calibration and efficiency uncertainty in the W boson mass is 9.8 MeV when estimated using the p_T^ℓ distribution and 9.7 MeV using m_T . The comparison in data and simulation of the dimuon invariant mass and the muon pseudorapidity distributions after applying corrections for momentum scale and resolution, and for reconstruction, isolation and trigger efficiencies, shows a very good agreement even in the tails of the mass lineshape.

The electron energy scale and resolution calibration uses Z boson events. The main difference with regards to the procedure used in the ATLAS Run 1 electron calibration paper¹¹ is the exclusion of the range $1.2 < |\eta| < 1.82$, as the amount of passive material in front of the calorimeter and its uncertainty are largest in this region. In addition, corrections are derived for the azimuthal variations of the electron-energy response due to gravity-induced mechanical deformations of the electromagnetic calorimeter, especially in the endcaps. Electron reconstruction, identification and trigger efficiency corrections are derived using $W \rightarrow e\nu$, $Z \rightarrow ee$ and $J/\psi \rightarrow ee$ events as a function of the electron p_T and η ¹⁴.

The comparison in data and simulation of the dielectron invariant mass and the electron pseudorapidity distributions in Z events, after applying corrections for energy scale, resolution and reconstruction, identification, isolation and trigger efficiencies, shows a very good agreement. The total systematic uncertainty due to the electron calibration and efficiency after combining the η categories is about 14 MeV on the W boson mass as derived from p_T^ℓ or m_T distributions.

3.2 Hadronic recoil calibration

The hadronic recoil has to be precisely calibrated, as it affects mostly the determination of the W boson mass through its impact on the m_T distribution where it enters directly in the definition of m_T , and only slightly for p_T^ℓ through the selection cuts. The hadronic recoil is highly sensitive to the pileup as well as to the underlying event activity. The calibration of the recoil corrects first for the modelling of the overall event activity in simulation, separately in the W and Z boson samples, which causes a recoil resolution mismodelling and as a second step for residual discrepancies in the recoil response and resolution derived using Z boson events in data, and transferred to the W boson sample. The uncertainties from the hadronic recoil calibration affect the W boson mass by 2.6 MeV when fitting the p_T^ℓ distribution and by 13 MeV for m_T .

3.3 Backgrounds in the W boson sample

Background contributions to the W boson event sample from Z boson, boson pair, $W \rightarrow \tau\nu$ and top-quark production are estimated using simulation. Contributions from multijet production are estimated with data-driven techniques. The estimation of the multijet background contribution follows similar procedures in the electron and muon decay channels, and relies on template fits to kinematic distributions in background-dominated regions. Three different observables, p_T^{miss} , m_T and p_T^ℓ/m_T , are used. Templates of the multijet background distributions for these observables are obtained from data by inverting the lepton energy-isolation requirements. The multijet background fraction is 0.6-1.7% and 0.5-0.7% depending on the η region in the electron channel and muon channel respectively.

4 Physics modelling

There is no single generator able to describe the various observed distributions. The simulated samples of inclusive vector-boson production are based on the Powheg MC generator interfaced to Pythia 8, henceforth referred to as Powheg+Pythia 8. Ancillary measurements of Drell–Yan

processes are used to validate (and tune) the model and to assess systematic uncertainties. The W and Z boson samples are reweighted to include the effects of higher-order QCD and EW corrections, as well as the results of fits to measured distributions which improve the agreement of the simulated lepton kinematic distributions with the data. The correction procedure is based on the factorisation of the fully differential leptonic Drell-Yan cross section into four terms:

$$\frac{d\sigma}{dp_1 dp_2} = \left[\frac{d\sigma(m)}{dm} \right] \left[\frac{d\sigma(y)}{dy} \right] \left[\frac{d\sigma(p_T, y)}{dp_T dy} \left(\frac{d\sigma(y)}{dy} \right)^{-1} \right] \left[(1 + \cos^2 \theta) + \sum_{i=0}^7 A_i(p_T, y) P_i(\cos \theta, \phi) \right], \quad (1)$$

where p_1 and p_2 are the lepton and anti-lepton four-momenta; m , p_T , and y are the invariant mass, transverse momentum, and rapidity of the dilepton system; θ and ϕ are the polar angle and azimuth of the lepton^ℓ in any given rest frame of the dilepton system; A_i are angular coefficients, and P_i are spherical harmonics of order zero, one and two.

The differential cross section as a function of the invariant mass, $d\sigma(m)/dm$, is modelled with the Breit-Wigner analytic formula. For the other terms, the signal simulation is reweighted according to various accurate predictions :

- The differential cross section as a function of rapidity, $d\sigma(y)/dy$, is modelled with perturbative QCD fixed-order NNLO prediction.
- The boson p_T at a given rapidity is modelled with Pythia 8 using the AZ tune¹⁵.
- The polarisation coefficients, A_i , are modelled with perturbative QCD fixed-order NNLO prediction.

4.1 Electroweak corrections

The dominant source of EW corrections originates from QED final-state radiation (FSR) and is included in the simulated samples with PHOTOS. The associated systematic uncertainties are negligible. The QED initial-state radiation (ISR) is included through Pythia 8 parton shower (PS). Pure weak corrections due to virtual-loop and box diagrams, interferences between QED FSR and ISR and final-state emissions of lepton pairs are not included in the simulation and are considered as systematic uncertainties. The total uncertainties are similar in the electron and muon channels and amount to about 5 MeV for p_T^ℓ and 3 MeV for m_T .

4.2 QCD corrections

Fixed-order predictions at NNLO are used to model the differential cross section as a function of boson rapidity and the angular coefficients as a function of the transverse momentum and rapidity of the boson. For the rapidity, the model is validated by checking its agreement with the 7 TeV ATLAS W and Z differential cross section measurements¹⁶. These data show a weaker suppression of strangeness compared to the u -, d -quark sea densities in the PDF, which motivates the choice of the CT10nnlo PDF set for the baseline model. The other PDF sets which show a reasonable agreement with the data, MMHT14nnlo and CT14nnlo, are used to assess the uncertainties.

The modelling of the A_i coefficients is validated by comparing with the 8 TeV measurement of the angular coefficients in Z boson decays¹⁷. The accuracy of the Z data is propagated as an uncertainty in the W boson mass. Good agreement between the measurements and the NNLO predictions is observed for the relevant angular coefficients, except for A_2 , for which the full

^aHere, lepton refers to the negatively charged lepton from a W^- or Z boson, and the neutrino from a W^+ boson.

discrepancy is taken as an uncertainty.

The W boson transverse momentum at a given rapidity is modelled with Pythia 8 PS generator. The QCD parameters of the PS model were determined by fits to the transverse momentum distribution of the Z boson measured at 7 TeV¹⁵. More advanced calculations, like resummed predictions (DYRES, CuTe, Resbos) and Powheg MinLO+Pythia 8, were tried but found to predict a much harder W boson transverse momentum for a given Z boson transverse momentum. To validate the choice of Pythia 8 as a reference model for the W boson mass measurement, the distribution of the parallel projection of the recoil along the lepton direction, a variable sensitive to p_T , is compared between data and the different predictions. These advanced calculations were strongly disfavoured by the data while PS predictions like Pythia 8, Herwig 7 and also Powheg+Pythia 8 show a very nice agreement.

To assess the systematic uncertainties from Z to W extrapolation, the ratio of boson transverse momenta is considered:

$$R_{W/Z}(p_T) = \left(\frac{1}{\sigma_W} \frac{d\sigma_W(p_T)}{dp_T} \right) \left(\frac{1}{\sigma_Z} \frac{d\sigma_Z(p_T)}{dp_T} \right)^{-1} \quad (2)$$

Uncertainties in the parton shower predictions include :

- accuracy of the Z data used in the Pythia 8 AZ tune
- c-quark and b-quark mass variations
- factorisation scale variation in the QCD ISR, decorrelating W and Z for the heavy flavour initiated production while correlating for the light quark production
- Leading order PS PDF variations, considering the maximum deviation on p_T^W/p_T^Z arising from different PDF sets compared to the nominal LO PDF set used in Pythia 8 CTEQ6L1: CT14lo, MMHT2014lo and NNPDF2.3lo PDF sets.

The uncertainty from the PDFs on the fixed-order predictions dominate the total uncertainty in the measurement and amounts to 8.0 MeV in the p_T^ℓ fit, and to 8.7 MeV in the m_T fit. These PDF variations are applied simultaneously to the boson rapidity, polarisation and transverse momentum. The PDF uncertainties are strongly anti-correlated between W^+ and W^- due to the fact that the total light-quark sea PDF is well constrained by deep inelastic scattering data, whereas the u-, d-, and s-quark decomposition of the sea is less precisely known.

5 Results

5.1 Z mass measurement

The detector response corrections and the physics modelling are validated by performing the measurement of the Z boson mass using the same method to determine the W boson mass and comparing it to the LEP combined value of $m_Z = 91187.5 \pm 2.1$ MeV. This method provides a closure test of the lepton calibration when using the lepton-pair invariant mass, and a test of the p_T dependence of the calibration and efficiency corrections and the modelling of the Z boson transverse momentum and of the relative fractions of Z boson helicity states when using p_T^ℓ . The extraction of m_Z from the m_T distribution, where it is defined in Z boson events by treating one of the reconstructed decay leptons as a neutrino, referred to as W-like Z boson mass measurement, checks the recoil calibration. The precision of this validation procedure is limited by the statistics of the Z boson sample. The combined extraction of m_Z from the p_T^ℓ distribution yields a result compatible with the LEP value within 0.9 standard deviations. The compatibility from the m_T distribution is about 1.5 standard deviations. The consistency tests based on the Z boson sample agree with the expectations within the uncertainties.

5.2 *W-like CMS Z boson mass measurement*

A similar Z boson mass measurement was performed by the CMS collaboration as a first milestone towards a W boson mass measurement. The analysis uses a sample of W-like events, i.e. $Z \rightarrow \mu\mu$ events where one of the muons has been removed to mimic the $W \rightarrow \mu\nu$ topology, in 2011 data at a centre-of-mass energy of 7 TeV. The phase space is defined by the following selection cuts: $30 < p_{\text{T}}^{\mu} < 55$ GeV, $30 < p_{\text{T}}^{\text{miss}} < 55$ GeV, $60 < m_{\text{T}} < 100$ GeV, $u_{\text{T}} < 15$ GeV and $p_{\text{T}}^Z < 30$ GeV. Muon momentum scale and resolution are calibrated using J/ψ and $\Upsilon(1S)$; an agreement at the 0.2 per mil level is achieved in the different η and p_{T}^{μ} bins. Half of the Z boson sample is used for hadronic recoil calibration and the second half for the fit of the W-like Z boson mass. The hadronic recoil is reconstructed from all the reconstructed charged tracks compatible with the primary vertex. This method has the advantage of being more pileup insensitive however shows a loss in the recoil response compared to the cluster-based method used in ATLAS. The W-like fits are performed in the ranges $32 < p_{\text{T}}^{\mu/\text{miss}} < 45$ GeV and $65 < m_{\text{T}} < 100$ GeV. The measured Z boson mass is in agreement with the LEP combined value within the statistical uncertainties which dominate this measurement. The lowest uncertainty is obtained when using the W^+ -like transverse mass, for which $M_Z^{\text{W-like}} = 91206 \pm 36$ (stat.) ± 30 (syst.) MeV.

5.3 *W boson mass measurement in ATLAS*

Before unblinding, the W boson mass was checked to be consistent in the different categories used for the measurement. In addition, the measurement was done using $p_{\text{T}}^{\text{miss}}$ distribution and in bins of pileup, recoil and u_{\parallel} , and by removing the $p_{\text{T}}^{\text{miss}}$ selection requirement. The stability of the result was also checked as a function of the charged-lepton azimuth and with respect to variations of the fitting ranges. The simulation was compared to data for the different control distributions and mass-sensitive variables and an overall good agreement was observed. The final combination of all categories gives consistent result with a χ^2/dof of 29/27, which indicates the accuracy of the experimental and theoretical modelling. The obtained result is:

$$m_W = 80370 \pm 7 \text{ (stat.)} \pm 11 \text{ (exp. syst.)} \pm 14 \text{ (mod. syst.) MeV.} \quad (3)$$

where the first uncertainty is statistical, the second corresponds to the experimental systematic uncertainty, and the third to the physics modelling systematic uncertainty. The final measurement uncertainty is dominated by modelling uncertainties, mainly the strong interaction uncertainties. Lepton calibration uncertainties are the dominant sources of experimental systematic uncertainty for the extraction of m_W from the p_{T}^{ℓ} distribution. The uncertainty in the recoil calibration dominates the experimental systematic uncertainty for the m_{T} distribution. In the final result, the muon decay channel has a weight of 57% and the p_{T}^{ℓ} dominates the measurement with a weight of 86%. Finally the charges contribute similarly with a weight of 52% for W^+ and of 48% for W^- . The result is compatible with the current world average and provides a world leading precision measurement together with the CDF collaboration. The different m_W results are compared in Figure 1, together with the SM prediction.

The dataset available at centre-of-mass energies of 8 and 13 TeV can be exploited to improve the precision of this measurement. An additional challenge with the increasing pileup will require more studies to achieve a more pileup-robust recoil resolution while preserving a good response. Further ancillary measurements can be used to provide more constraints on the PDFs and to improve the QCD and EW predictions for Drell–Yan production. Moreover more work is needed on the theory side to reduce the modelling uncertainties and to provide a single tool with an accurate advanced computation.

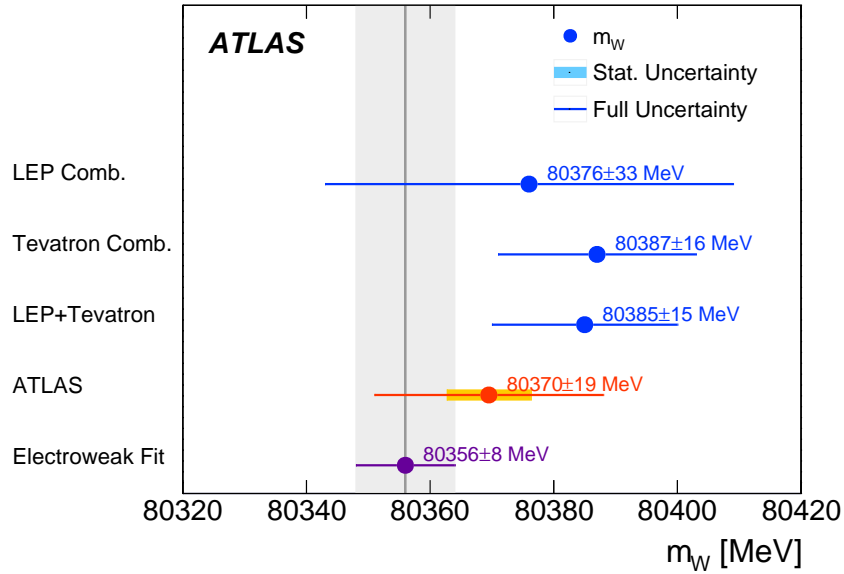


Figure 1 – The W boson mass measured in ATLAS is compared to the combined measurements in LEP and Tevatron experiments, and to the SM prediction from the EW fit⁸.

References

1. S. L. Glashow, Nucl. Phys. **22**, 579 (1961).
2. A. Salam and J.C. Ward, Phys. Lett. **13** 168 (1964).
3. S. Weinberg, Phys. Rev. Lett. **19**, 1264 (1967).
4. M. Baak *et al.*, Eur. Phys. J. C **74**, 3046 (2014).
5. Particle Data Group, K. A. Olive *et al.*, Chin. Phys. C **38**, 090001 (2014).
6. T. Aaltonen *et al.*, Phys. Rev. Lett **108**, 151803 (2012).
7. ATLAS Collaboration, JINST 3 S08003 (2008).
8. ATLAS Collaboration, arXiv:1701.07240 [hep-ex].
9. CMS Collaboration, JINST 3 S08004 (2008).
10. CMS Collaboration, CMS PAS SMP-14-007.
11. ATLAS Collaboration, Eur. Phys. J. C **74**, 3071 (2014).
12. ATLAS Collaboration, Eur. Phys. J. C **74**, 3130 (2014).
13. S. Schael *et al.*, Phys. Rept **427**, 257 (2006).
14. ATLAS Collaboration, Eur. Phys. J. C **74**, 2941 (2014).
15. ATLAS Collaboration, JHEP **09**, 145 (2014).
16. ATLAS Collaboration, arXiv:1612.03016 [hep-ex].
17. ATLAS Collaboration, JHEP **08**, 159 (2016).